Solvent-Mediated Folding of a Doubly Charged Anion

Xin Yang,[1,2] You-Jun Fu,[1,2] Xue-Bin Wang,[1,2] Petr Slavicek,[3] Martin Mucha,[3] Pavel Jungwirth,[3*] Lai-Sheng Wang[1,2*]

[1]*Department of Physics, Washington State University, 2710 University Drive, Richland, WA 99352, USA and*

[2]*W. R. Wiley Environmental Molecular Sciences Laboratory, Pacific Northwest National Laboratory, P.O. Box 999, Richland, WA 99352, USA*

[3]*J. Heyrovsky Institute of Physical Chemistry, Academy of Sciences of the Czech Republic and Center for Complex Molecular Systems and Biomolecules, Dolejskova 3, 18223 Prague 8, Czech Republic*

***To whom correspondence should be addressed. E-mails: pavel.jungwirth@jh-inst.cas.cz and ls.wang@pnl.gov**

Abstract

The microsolvation of the suberate dianion, $^{-}O_2C(CH_2)_6CO_2^{-}$, with two separate charge centers was studied by photoelectron spectroscopy and molecular dynamics simulation one solvent molecule at a time for up to 20 waters. It is shown that the two negative charges are solvated in the linear suberate alternately. As the solvent number increases, the negative charges are screened and a conformation change occurs at 16 waters, where the cooperative hydrogen-bonding of water is large enough to overcome the Coulomb repulsion and pull the two negative charges closer through a water bridge. This conformation change, revealed both from the experiment and simulation, is a manifestation of the hydrophilic and hydrophobic forces at the molecular level.

Introduction

Understanding the behavior of ions, especially multiply-charged species, in aqueous solution is essential to obtain insight into many processes in chemistry and biochemistry. Many textbook multiple-charged anions (MCAs), such as SO_4^{2-}, own their existence to their hydration shell and would spontaneously emit an electron in free space.[1,2] For biological macromolecules, solvation of their charged groups plays an important role in determining their structures and functions.[3-5] Studying the microhydration of complex multiply-charged anions in the gas phase provides a unique vantage point to understand at the molecular level the solvation effect on the structure of the solute molecules.

Photoelectron spectroscopy (PES) is a sensitive probe for the solvation environment of MCAs and their intramolecular electrostatic interactions. We have developed an experimental technique to study gaseous MCAs using electrospray ionization (ESI) and PES.[6] The ESI technique is a powerful soft ionization method to produce MCAs, as well as any ionic species and solvated clusters from solution to the gas phase.[7-10] Using these techniques, we have investigated the hydration of two common inorganic dianions, SO_4^{2-} and $C_2O_4^{2-}$, with up to 40 water molcules[11-14] and a series of dicarboxylate dianions, $^-O_2C\text{-}(CH_2)_x\text{-}CO_2^-$ (x = 2-10) with one and two water molecules.[15]

Carboxylate is an important negative charge carrier in proteins, present in the C-terminal of polypeptides and the side chains of aspartic and glutamic acids. Linear dicarboxylate dianions $^-O_2C\text{-}(CH_2)_n\text{-}CO_2^-$ have two distinct charged groups ($\text{-}CO_2^-$) linked by a flexible aliphatic chain and can be viewed as a simple model for peptide chains. Here we report the first observation of solvent-mediated folding of suberate dianion $^-O_2C\text{-}(CH_2)_6\text{-}CO_2^-$. We studied the microsolvation of the suberate dianion using PES and molecular dynamics simulations. We observed that water molecules solvate the two negative charges in the linear suberate alternately at the two ends, but not the middle hydrophobic aliphatic chain. As the solvent number increases, the negative charges are screened and a folding occurs at about 16 waters, where the cooperative hydrogen-bonding of water is large enough to overcome the Coulomb repulsion and pull the two negative

charges closer through a water bridge. The current work provides a simple and clean model system to study the hydrophilic and hydrophobic effects,[16-17] as well as solvent-mediated formation of like-ion pairs in solution,[18-20] and is likely to be important for understanding the hydration and conformation changes of biological molecules.[21-23]

Experimental Methods

The experiment was carried out using an experimental apparatus equipped with a magnetic-bottle time-of-flight photoelectron analyzer and an ESI source. Details of the experimental method have been given elsewhere.[6] Briefly, solvated suberate dianions with a wide range of solvent number, $^{-}O_2C(CH_2)_6CO_2^{-}(H_2O)_n$, were produced from electrospray of a mixed solution of 10^{-3} M suberic acid and 2×10^{-3} M NaOH in water-acetonitrile (1:4 volume ratio). Anions produced from the ESI source were guided into a room-temperature ion-trap, where ions were accumulated for 0.1 second before being pulsed into the extraction zone of a time-of-flight mass spectrometer.

During the PES experiment, the bare and solvated suberate dianions were mass-selected and decelerated before being intercepted by a probe laser beam in the photodetachment zone of the magnetic-bottle photoelectron analyzer. In the current study, the detachment photon energy used was 193 nm (6.424 eV). Experiments were performed at 20 Hz repetition rate with the ion beam off at alternating laser shots for background subtraction, which was critical for high photon energy experiments due to background noises. Photoelectrons were collected at nearly 100% efficiency by the magnetic-bottle and analyzed in a 4-meter long electron flight tube. Photoelectron time-of-flight spectra were collected and then converted to kinetic energy spectra, calibrated by the known spectra of I^- and O^-. The electron binding energy spectra presented here were obtained by subtracting the kinetic energy spectra from the detachment photon energies. The energy resolution ($\Delta E/E$) was about 2%, i.e., ~10 meV for 0.5 eV electrons, as measured from the spectrum of I^- at 355 nm.

Theoretical Methods

The calculations involved a combination of classical molecular dynamics simulations aimed at a Boltzmann sampling of geometries of the $^{-}O_2C(CH_2)_6CO_2^{-}(H_2O)_n$ clusters and ab initio quantum chemistry for evaluation of detachment energies. Very long (microsecond) simulations were performed at constant temperatures (ranging from 150 to 230 K) with a time step of 1 fs. Note that at these temperatures the cluster is not solid but liquid-like and rather flexible, which is both due to the presence of the suberate dianion and the small size of the system. We employed the SPCE model of water,[24] while for the suberate dianion, we used the Cornell force field[25] with fractional charges evaluated at the HF/6-31G* level. All molecular dynamics calculations were performed using the GROMACS 3.1 program package.[26]

Ab initio calculations were used to evaluate the vertical detachment energies (VDE) of $^{-}O_2C(CH_2)_6CO_2^{-}(H_2O)_n$ (n = 0-25). While for geometry parameters the Hartree-Fock method performed satisfactorily, correlation effects had to be included for reliable calculations of the VDEs. From the basis set point of view, a modest 6-31$_{+O}$G* provided already almost converged results. For the bare suberate dianion and small clusters, we calculated their VDEs using CCSD(T)/6-31$_{+O}$G* and MP2 levels of theory. For larger clusters, explicit inclusion of water molecules into the ab initio calculation became computationally unfeasible. We, therefore, replaced the water molecules by fractional charges of -0.82 e (oxygen) and +0.41 e (hydrogen). This replacement almost did not change the value of VDEs, e.g., the increase of VDE of suberate by two water molecules changed from 0.83 to 0.89 eV by this procedure. All ab initio calculations were performed using the Gaussian 98 program.[27]

Experimental Results

Mass Spectra. Typical mass spectra of $^{-}O_2C(CH_2)_6CO_2^{-}(H_2O)_n$ from our ESI source are shown in Figure 1. Due to the perpendicular extraction configuration of ions in our time-of-flight mass spectrometer, we can only optimize ion signals for a limited mass range. Figure 1 shows

three separately optimized mass spectra, covering the full mass range of interest currently. Solvated suberate dianion clusters with up to 30 water molecules were readily produced. In general, the mass intensities of $^{-}O_2C(CH_2)_6CO_2^{-}(H_2O)_n$ decreased monotonically as *n* increased. Strong mass signals of two singly charged ion pairs, $NaO_2C(CH_2)_6CO_2^{-}$ and $HO_2C(CH_2)_6CO_2^{-}$ were observed, as labeled in the second panel of Figure 1. Most of the unlabeled mass peaks were due to the mixed solvent species, $^{-}O_2C(CH_2)_6CO_2^{-}(H_2O)_x(CH_3CN)_y$.

Photoelectron Spectra. Figure 2 displays the photoelectron spectra of $^{-}O_2C(CH_2)_6CO_2^{-}(H_2O)_n$ for *n* = 0-20. The two intense overlapping bands in the spectrum of the bare dianion were due to electron detachment from the $-CO_2^{-}$ groups.[28] The small bump centered at ~4.6 eV was due to detachment of singly charged anions by a second photon. Several observations can be made about the spectra of the small solvated species (*n* = 1-9). First, the electron binding energies increase as a function of solvent number due to stabilization of the negative charges by water. Second, the spectral features showed an odd-even effect: those with even solvent numbers were similar to those of the bare dianion while those with odd solvent numbers exhibit an extra band. Third, for $n \geq 2$, a new band emerged at the high binding energy side. Its relative intensity reached the maximum at *n* = 4, then decreased gradually and disappeared for $n > 8$. Similar spectral features were observed in the our previous PES studies of $SO_4^{2-}(H_2O)_n$, $C_2O_4^{2-}(H_2O)_n$ and $F^{-}(H_2O)_n$ systems and they were found to be due to ionization of the solvent.[12-14,29] The ionization potential of water was significantly lowered in the presence of the negative ions due to the strong Coulomb repulsion. Forth, spectral features on the high binding energy side were cut off as a result of the repulsive Coulomb barrier (RCB), which exists universally in multiply charged anions and essentially prohibits slow electrons from being emitted.[28] The cutoff point in each spectrum provides a rough estimate of the barrier height (photon energy minus the cutoff energy), which has been shown to be approximately equal to the magnitude of the intramolecular Coulomb repulsion.[28]

For the large solvated clusters (*n* = 10-20), the even-odd effect of the spectral features became smeared out. With increasing solvent number, the spectral features moved steadily to

high binding energies until n = 16, where the spectrum suddenly shifted to lower binding energies. For n>16, the spectral features moved again to high binding energies. Beside the sudden change of the binding energies, we also observed a backward shift of the spectral cutoff. The cutoff, which increased slowly with the solvent number for n<16, is clearly shifted to lower binding energies in the spectra of n>16 relative to those of n<16, giving rise to the appearance of a sharper peak for these large clusters.

Adiabatic and Vertical Detachment Energies. The adiabatic detachment energy (ADE) and VDE determined from the spectrum of each cluster are listed in Table 1. Due to the lack of vibrational resolution, the ADEs were measured by drawing a straight line along the leading edge of the threshold band and then adding a constant to the intersection with the binding energy axis to take into account the instrumental resolution at the given energy range. Despite the approximate nature of this procedure, a consistent set of ADEs with reasonable uncertainties could be obtained. The VDE was measured from the maximum of the first band. However, due to the overlap between the first band and the higher binding energy band in the large solvated clusters, the VDEs could not be determined precisely, as reflected by the large uncertainties given for the reported VDEs in Table 1.

The measured ADEs are also plotted in Figure 3A (the blue curve) as a function of solvent number. The odd-even effect and the sudden drop of ADE at n = 16 are revealed readily. These effects can be seen more dramatically in Figure 3B, which showed the differential ADE [ΔADE = ADE(n) - ADE(n-1)] as a function of solvent number. The ADE of n = 16 shows a decrease of ~0.3 eV relative to that of n =15.

V. Discussion

Solvation at Linear Conformation. The suberate dianion has two equivalent -CO_2^- groups. The Coulomb repulsion between the two charges keeps them as far as possible from each other in the free dianion, i.e., in a quasi-linear conformation, as we showed previously.[28] For small solvated clusters, both the PES features and the electron binding energies show clearly an

odd-even effect (Figures 2 and 3). This observation suggests that the solute dianion maintains its linear conformation in the small solvated clusters and the two $-CO_2^-$ groups are solvated alternately with increasing solvent number: the first water solvates one of the two $-CO_2^-$ groups on one end of the suberate dianion, while the second water solvates the other one independently. Because for $n = 1$ only one side of the dianion is solvated leaving the other $-CO_2^-$ group relatively unaffected, it is understandable that only a small increase of ADE (0.19 eV) was observed relative to the bare suberate dianion. For $n = 2$, both $-CO_2^-$ groups are stabilized by one water, resulting in an extremely large ΔADE (0.62 eV), as shown in Figure 3B. For even solvent numbers the two negative charges are solvated symmetrically and maintain their equivalence. Thus their PES spectra are similar to that of the bare dianion. For odd solvent numbers, however, the two charges are solvated asymmetrically and become inequivalent, thus giving rise to the extra band in their PES spectra. The odd-even effect becomes smeared out beyond $n = 9$ because the inequivalence due to the difference of one water becomes insignificant.

Control Experiments. The observation of a decrease in ADE at $n = 16$ in the hydrated suberate was totally unexpected. In all previous PES studies of solvated anions,[11-14,30,31] the ADEs were always observed to increase with solvent numbers. A decrease of ADE with increasing solvent numbers has never been observed before. To confirm our observation, we performed two control experiments using two isomers of the benzene-dicarboxylate (BDC), in which the $-CO_2^-$ groups are connected by the rigid phenyl ring. The first experiment was the hydrated *o*-BDC dianions, in which the two $-CO_2^-$ groups are next to each other. The ADEs of the hydrated *o*-BDC in the same range of solvent numbers (n = 0-20) are also plotted in Figure 3A (the green curve). In contrast to the hydrated suberate dianions, no odd-even effect was observed (Figure 3B, the green curve) because each solvent molecule can interact with the two $-CO_2^-$ groups at the same time due to their proximity. Our second control experiment used hydrated *p*-BDC, in which the two $-CO_2^-$ groups are on the opposite site of the phenyl ring in a linear configuration. The ADEs of the hydrated *p*-BDC (Figure 3A, red curve) are higher than those of the *o*-BDC due to the reduced Coulomb repulsion. Unlike the *o*-BDC system the

hydrated *p*-BDC dianions displayed an odd-even effect (Figure 3B, red curve), because water solvates the two carboxylate groups in *p*-BDC separately and independently in a similar fashion as in the hydrated suberate. The magnitude of the odd-even effect is much smaller for the *p*-BDC system because the aromatic phenyl ring between two charges is much more polarizable than the aliphatic chain in suberate. However, both the *o*-BDC and *p*-BDC systems exhibit only a monotonic increase in their ADEs as a function of solvent number and no drop was observed at $n = 16$ (Figure 3A).

Solvent-Mediated Folding. Thus, the ADE decrease at $n = 16$ for the hydrated suberate must indicate a conformation change of the dianion caused by solvation. In contrast to the rigid phenyl ring, the aliphatic chain in the suberate is flexible. As water is added one molecule at a time, there are two major forces acting in the hydrated dianions: the Coulomb repulsion and the hydrophilic hydration. The Coulomb repulsion dominates in the bare dianion and smaller hydrated clusters, keeping the two negative charges as far as possible in the linear confirmation. The first few waters provide enormous stabilization to the negative charges, on average by ~0.4 eV per water for the first four waters in all three dicarboxylates (Figure 3B). As the negative charges are further solvated, the stabilization of adding an extra water steadily decreases. Beyond $n = 8$, the differential ADE is less than 0.2 eV and drops to about 0.1 eV per water for $n>12$ (Figure 3B). This is because the negative charges become fully solvated at certain solvent number, and additional waters have no direct interactions with them.

As more water is added, the two negative charges are screened and it becomes thermodynamically less favorable to have two separate solvation centers. The merge of the two separated water droplets would result in a significant energy gain due to the cooperative hydrogen-bonding effect in the resulting larger water droplet. However, the formation of a single water droplet would require pulling the two negative charges closer and excluding the hydrophobic aliphatic chain by folding. This causes unfavorable Coulombic interaction between the two negative charges in the folded conformation. Hence the merging of the two water droplets only becomes possible when there are enough water molecules to provide a sufficiently

high stabilization due to the cooperative hydrogen-bonding to overcome the resulting increase in Coulomb repulsion. For suberate, our data suggest this happens at $n \sim 16$. The extra Coulomb repulsion upon folding can be estimated to be approximately the ADE drop from $n = 15$ to 16, i.e., ~0.3 eV. Thus, the cooperative hydrogen-bonding effect resulting from the merge of the two water droplets must be higher than 0.3 eV.

The increase of Coulomb repulsion in the hydrated suberate for $n>16$ can also be inferred from the spectral cutoff in the PES spectra (Figure 2).[28] This cutoff is clearly shifted to lower binding energies in the spectra of $n>16$ relative to those of $n<16$, indicating that the RCB in the larger solvated clusters has increased. We note that in the spectrum of $n = 15$, there is a small tail at the lower binding energy side, which could indicate that there might already be a small population of folded clusters. The fact that the spectral cutoff of $n = 16$ is similar to that of $n = 15$ also suggests that there might be a small amount of linear isomers in the $n = 16$ solvated clusters. But for $n = 17$ and higher, the folded isomers seem to dominate.

NMR experiments on the hydration of polypeptides[32] showed that the aspartate and glutamate anions (each contains one $-CO_2^-$ group) are commonly hydrated by 6 or 7 waters under normal solution conditions at -35 °C and pH 6-9. These numbers are strikingly similar to our current observations, implying that folding only occurs once each carboxylate is fully hydrated and screened.

Molecular Dynamics Simulations. Molecular dynamics simulations at the microsecond time scale confirm the above interpretation of the PES spectra in terms of folding of the suberate dianion upon solvation, and the consequent close approach of the two anionic centers and the merge of the two water structures around them. Our simulations revealed that the folding depends on both the cluster size and temperature. In Figure 4A, we show the distribution of distances between the carbon atoms of the two $-CO_2^-$ groups of the dianion for $n = 15$ at 230 K. This distribution strongly peaks around 9 , which is a clear signature of the linear suberate dianion. There is also a very weak signal at around 5.5 , which corresponds to the folded geometries. A very similar picture emerges from a simulation for $n = 18$ at the same temperature,

as depicted in Figure 4B. Upon further solvation, however, the folded geometries start to be significantly populated, as shown by the rise of a peak around 5.5 for n = 21 (Figure 4C). We see in Figure 4C a co-existence of folded (5.5Å) and linear (9Å) structures with small fractions of almost unfolded (7-8Å) geometries. Further increasing the cluster size to 24 waters leads to a continuing population shift towards the folded geometries (Figure 4D), such that at this cluster size the folded structures clearly dominate. These simulation results are already in qualitative agreement with the PES observation.

In order to assess the influence of temperature we also performed simulations at 150 K. Unlike the run at 230 K, we were not able to obtain fully thermodynamically converged results within a microsecond simulation due to increasing non-ergodicity of the system at 150 K. Nevertheless, the results indicate that the effect of decreasing temperature is non-negligible, shifting the critical cluster size for folding to smaller values. While at 230 K folding of the suberate dianion only starts around n = 15-18, at 150 K clusters of these sizes have already significant fractions of folded structures. Clearly, the entropy term, which is more important at higher temperatures, shifts the balance towards the more floppy linear geometries, disfavoring the more rigid folded structures. Note that the temperatures of the clusters in the experiment were not precisely defined. However, due to evaporative cooling during the long trapping time (~0.1 second) the cluster temperatures could lie significantly below the room temperature, at which the ion trap was held. On the basis of a previous estimate of protonated water clusters under evaporative cooling,[33] the temperatures of our hydrated suberate clusters could be below 200 K. Within this uncertainty we conclude that the simulation results not only confirm the above interpretation of the solvent-induced folding based on the PES data, but are also in quantitative agreement with the experimental observations.

Figure 5 shows snapshots from the molecular dynamics simulations for several clusters. The first three snapshots display an unfolded suberate dianion for n = 1, 2, 15. The last snapshot (Figure 4D) shows a folded suberate dianion fro n = 18. Comparing Figure 5C and 5D we see that for the linear structure a separate water cluster is formed around each of the two -

CO_2^- groups, while in the folded structure a single water cluster is formed, bringing to close contact the two anionic centers. In the supplementary materials, we include two short movies made from the simulation, showing how a linear solvated suberate comes to the folded configuration at two solvent numbers and two different temperatures.

Ab Initio Calculations. To further support this interpretation, we carried out additional ab initio calculations for the VDEs. At the CCSD(T)/6-31$_{+O}$G* level. the VDE of the bare suberate dianion amounts to 1.63 eV, which compares favorably with the experimental value (1.86 eV, Table 1), while at the MP2 level the value is only 1.14 eV. However, the differential detachment energies between clusters with different numbers of water molecules are well described already at the MP2 level, presumably due to the dominant electrostatic effect. For example, two water molecules increase the MP2 VDE by 0.83 eV compared to the bare suberate, the experimental value being 0.85 eV (Table 1). We evaluated the differences between VDEs for a set of 20 folded, 20 linear, and 12 almost unfolded structures for n = 21, taken from the simulations. Although the VDEs in each set exhibit a certain spread (~0.2 eV), the detachment energies for the set of folded geometries lie on average 0.5 eV (or 0.4 eV) below those of the linear (or almost unfolded) structures. The 0.5 eV decrease in VDE of the folded structures is due to the increased Coulomb repulsion between the two negative charges relative to the linear isomers. This theoretical result confirms the PES observation that the decrease of detachment energies at n = 16 signified a conformation change .

Despite the increase of intramolecular Coulomb repulsion in the folded structure, the total energy of the system is decreased due to the enhanced solvent interaction, giving the appearance of an attraction between the two negative charges as they are pulled closer in the folded conformation. Thus, the solvated suberate dianions not only provide a detailed molecular picture of hydrophilic and hydrophobic salvation, but also demonstrate how these forces operate synergically to dictate the molecular configuration and give rise to an overall effective attractive interaction between the two negative charges.

Conclusions

Using photoelectron spectroscopy and molecular dynamics simulation, we studied the microsolvation of the suberate dianion, $^{-}O_2C(CH_2)_6CO_2^{-}$, one solvent molecule at a time for up to 20 waters. Both the PES spectral feature and the ADE show an odd-even effect revealing that the suberate dianion keeps its linear conformation in the small solvated clusters, and water molecules solvate the two negative charges alternately and independently at the two ends. As the solvent number increased, we observed surprisingly that the ADE for suberate solvated with 16 water molecules decreased relative that for the 15-water solvated suberate, indicating a solvent-mediated conformation change. For the large solvated clusters, the negative charges are screened and a folding occurs at 16 waters, where the cooperative hydrogen-bonding of water is large enough to overcome the Coulomb repulsion and pull the two negative charges closer through a water bridge. Molecular dynamics simulations and ab initio calculations confirmed the experimental observations and further revealed the temperature effect on the critical size for folding. We found that at higher temperatures the critical size for folding shifts to larger solvent numbers due to the entropic effect, which is more important at higher temperatures. The current experimental and theoretical methods provide a new tool to probe solvent-mediated conformation changes and the electrostatic environments in multiply-charged macromolecules, and hydrophobic and hydrophilic interactions at a molecular level.[21-23,34,35]

Acknowledgments. This work was supported by the U.S. Department of Energy (DOE), Office of Basic Energy Sciences, Chemical Science Division and performed at EMSL, a national scientific user facility sponsored by DOE s Office of Biological and Environmental Research and located at Pacific Northwest National Laboratory, operated for DOE by Battelle. Support (to P.J.) from the Czech Ministry of Education (Grant LN00A032) and the National Science Foundation (Grant CHE-0209719) is gratefully acknowledged.

Supplementary Information: Two short movies showing the folding of a linear suberate dianion with 18 water molecules at 150 K and 24 water molecules at 230 K.

References

1. Boldyrev, A. I.; Simons, J. *J. Phys. Chem*. **1994**, *98*, 2298.
2. Wang, X. B.; Nicholas, J. B.; Wang, L. S. *J. Chem. Phys*. **2000**, *113*, 10837.
3. Ohtaki, H.; Radnai, T. *Chem. Rev*. **1993**, *93*, 1157.
4. Israelachvili, J.; Wennerstrom, H. *Nature* **1996**, *379*, 219.
5. Otting, G.; Liepinsh, E.; W thrich, K. *Science* **1991**, *254*, 974.
6. Wang, L. S.; Ding, C. F.; Wang, X. B.; Barlow, S. E. *Rev. Sci. Instrum*. **1999**, *70*, 1957.
7. Blades, A. T.; Kebarle, P. *J. Am. Chem. Soc.* **1994**, *116*, 10761.
8. Baldes, A. T.; Klassen, J. S.; Kebarle, P. *J. Am. Chem. Soc.* **1995**, *117*, 10563.
9. Blades, A. T.; Ho, Y.; Kebarle, P. *J. Phys. Chem*. **1996**, *100*, 2443.
10. Lau, T. C.; Wang, J.; Guevremont, R.; Siu, K. W. M. *J. Chem. Soc., Chem. Commun*. 1**995**, 877.
11. Wang, X. B.; Nicholas, J. B.; Wang, L. S. *J. Chem. Phys*. **2000**, *113*, 10837.
12. Wang, X. B.; Yang, X.; Nicholas, J. B.; Wang, L. S. *Science* **2001**, *294*, 1322.
13. Yang, X.; Wang, X. B.; Wang, L. S. *J. Phys. Chem. A* **2002**, *106*, 7607.
14. Wang, X. B.; Yang, X; Nicholas, J. B.; Wang, L. S. *J. Chem. Phys*. **2003**, *119*, 3631.
15. Ding, C. F.; Wang, X. B.; Wang, L. S. *J. Phys. Chem. A* **1998**, *102*, 8633.
16. Ben-Naim, A. *Hydrophobic Interactions* (Plenum Press, New York, **1980**).
17. Cheng, Y. K.; Rossky, P. J. *Nature* **1998**, *392*, 696.
18. Pettitt, B. M.; Rossky, P. J. *J. Chem. Phys*. **1986**, *84*, 5836.
19. Jungwirth, P.; Zahradnik, R. *J. Phys. Chem*. **1994**, *98*, 1328.
20. Wallqvist, A.; Covell, D. G. *J. Phys. Chem*. **1995**, *99*, 5705.
21. Makarov, V.; Pettitt, B. M.; Feig, M. *Acc. Chem. Res*. **2002**, *35*, 376.
22. Gross, D. S.; Schnier, P. D.; Rodriguez-Cruz, S.E.; Fagerquist, C. K., Williams, E. R. *Proc. Natl. Acad. Sci*. (USA) **1996**, *93*, 3143.
23. Jarrold, M. F. *Acc. Chem. Res*. **1999**, *32*, 360.
24. Berendsen, H. J. C., Grigera, J. R. & Straatsma, T. P. *J. Phys. Chem.* **1987**, 91, 6269.

25. Cornell, W. D., Cieplak, P., Bayly, C. I., Gould, I. R., Merz Jr., K. M., Ferguson, D. M., Spellmeyer, D. C., Fox, T., Caldwell, J. W. & Kollman, P. A. *J. Am. Chem. Soc.* **1995**, *117*, 5179.

26. Lindahl, E., Hess, B. & van der Spoel, D. *J. Mol. Mod*. **2001**, *7*, 306.

27. Frisch, M. J. *et al*. *Gaussian 98* (Gaussian, Inc., Pittsburgh PA, **1998**).

28. Wang, L. S., Ding, C. F., Wang, X. B., Nicholas, J. B. *Phys. Rev. Lett*. **1998**, *81*, 2667.

29. Yang, X; Wang, X. B.; Wang, L. S. *J. Chem. Phys*. **2001**, *115*, 2889.

30. Markovich, G., Pollack, S., Giniger, R. & Cheshnovesky, O. *J. Chem. Phys*. **1994**, *101*, 9344.

31. Coe, J. V., Earhart, A. D., Cohen, M. H., Hoffman, G. J., Sarkas, H. W. & Bowen, K. H. *J. Chem. Phys*. **1997**, *107*, 6023.

32. Kuntz, I.D. *J. Am. Chem. Soc*. **1971**, *93*, 514.

33. Klots, C. E. *J. Chem. Phys.* 1985, *93*, 5854.

34. Pratt, L. R.; Phohorille, A. *Chem. Rev*. 2002, *102*, 2671.

35. Sorenson, J. M., Hura, G., Soper, A. K., Pertsemlidis, A. & Head-Gordon, T. *J. Phys. Chem*. B 1999, *103*, 5413.

Table 1. The experimental adiabatic (ADE), vertical (VDE) detachment energies of $^-O_2C(CH_2)_6CO_2^-(H_2O)_n$.

Solvent Number	ADE (eV)	VDE (eV)
0	1.55 ± 0.05	1.86 ± 0.06
1	1.74 ± 0.05	2.02 ± 0.06
2	2.36 ± 0.05	2.71 ± 0.06
3	2.53 ± 0.05	2.81 ± 0.06
4	2.96 ± 0.05	3.3 ± 0.1
5	3.07 ± 0.06	3.4 ± 0.1
6	3.35 ± 0.06	3.8 ± 0.1
7	3.50 ± 0.06	3.9 ± 0.1
8	3.72 ± 0.06	4.2 ± 0.1
9	3.80 ± 0.06	4.3 ± 0.2
10	3.96 ± 0.06	4.5 ± 0.2
11	4.07 ± 0.08	4.6 ± 0.2
12	4.23 ± 0.08	4.9 ± 0.2
13	4.34 ± 0.08	5.0 ± 0.2
14	4.39 ± 0.08	5.0 ± 0.2
15	4.41 ± 0.08	5.1 ± 0.2
16	4.13 ± 0.08	4.7 ± 0.2
17	4.20 ± 0.08	4.8 ± 0.2
18	4.3 ± 0.1	5.0 ± 0.2
19	4.4 ± 0.1	5.1 ± 0.2
20	4.5 ± 0.1	5.2 ± 0.2

Figure Captions

Figure 1. Typical mass spectra of $^{-}O_2C(CH_2)_6CO_2^{-}(H_2O)_n$ from electrospray ionization of a suberate solution and optimized for three mass ranges. $H[DA]^-$ and $Na[DA]^-$ indicate the singly charged protonated and sodiated suberate ion pairs, respectively.

Figure 2. Photoelectron spectra of $^{-}O_2C(CH_2)_6CO_2^{-}(H_2O)_n$ (n = 0-20) at 193 nm (6.424 eV).

Figure 3. Comparisons of the adiabatic electron detachment energies (ADE) of $^{-}O_2C(CH_2)_6CO_2^{-}(H_2O)_n$ (n = 0-20) with those of p-$C_6H_4(CO_2^{-})_2$ (n = 0-20) and o-$C_6H_4(CO_2^{-})_2$ (n = 0-20). **(A)** The ADE as a function of solvent number (n). **(B)** Differential ADE, defined as $\Delta ADE = ADE(n) - ADE(n\text{-}1)$. Blue curve -- hydrated suberate; red curve -- hydrated p-benzene dicarboxylate; green curve -- hydrated o-benzene dicarboxylate.

Figure 4. Distributions of distances between the carbon atoms of the two $-CO_2^-$ groups of hydrated suberate at 230 K. **(A)** Suberate with 15 water molecules. **(B)** Suberate with 18 water molecules. **(C)** Suberate with 21 water molecules. **(D)** Suberate with 24 water molecules. Note the appearance and rise of folded suberate (peak around 5.5) and decrease of unfolded suberate (peak around 9) upon increasing solvent number.

Figure 5. Snapshots from simulations of the suberate dianion in selected water clusters. **(A)** Suberate with one water molecule. **(B)** Suberate with two water molecules. **(C)** Suberate with fifteen water molecules. **(D)** Suberate with eighteen water molecules (folded structure).

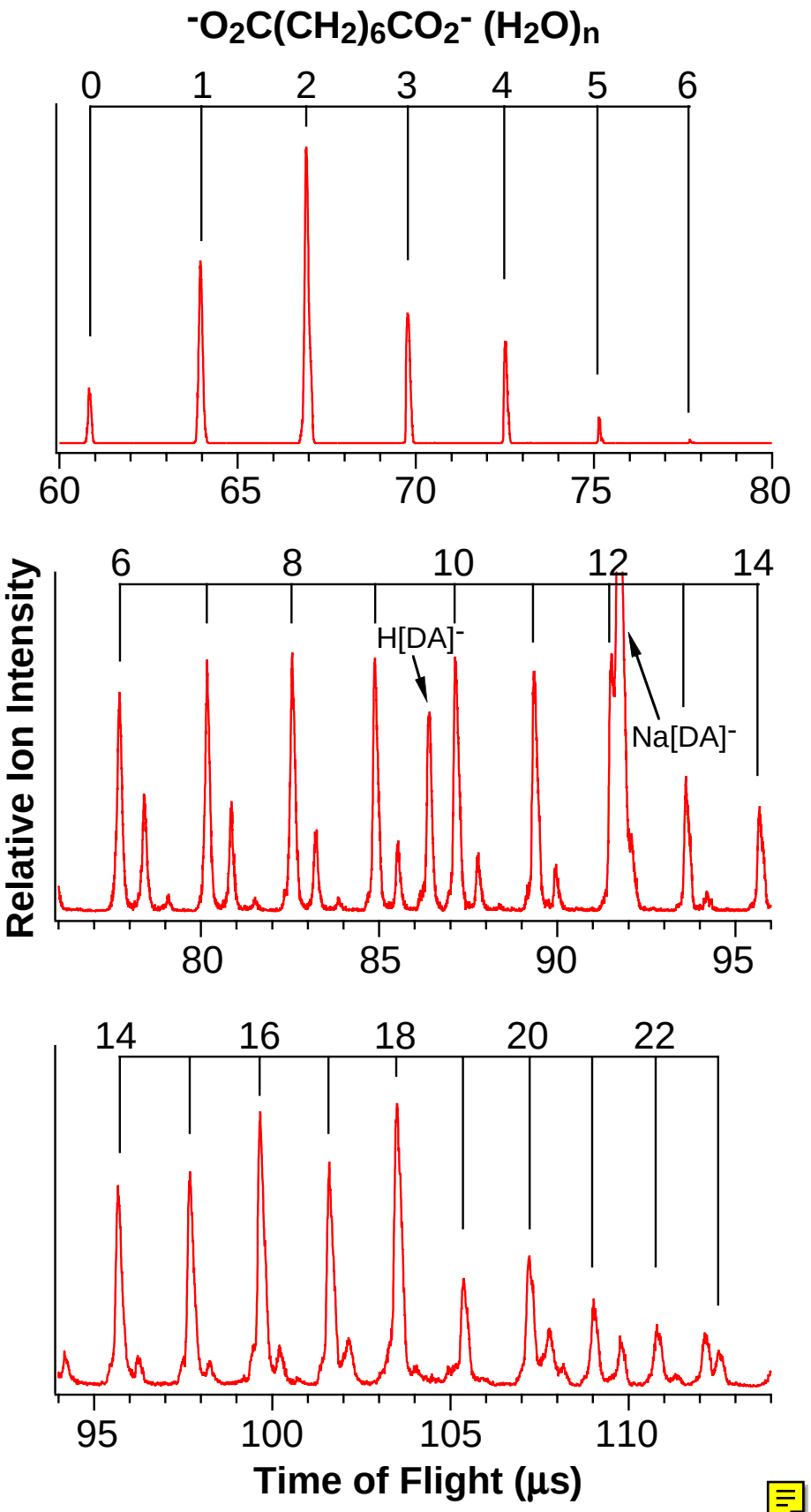
$^{-}O_2C(CH_2)_6CO_2^{-}$ $(H_2O)_n$
0
1
2
3
4
5
6
60
65
70
75
80
6
8
10
12
14
H[DA]$^{-}$
Na[DA]$^{-}$
Relative Ion Intensity
80
85
90
95
14
16
18
20
22
95
100
105
110
Time of Flight (μs)

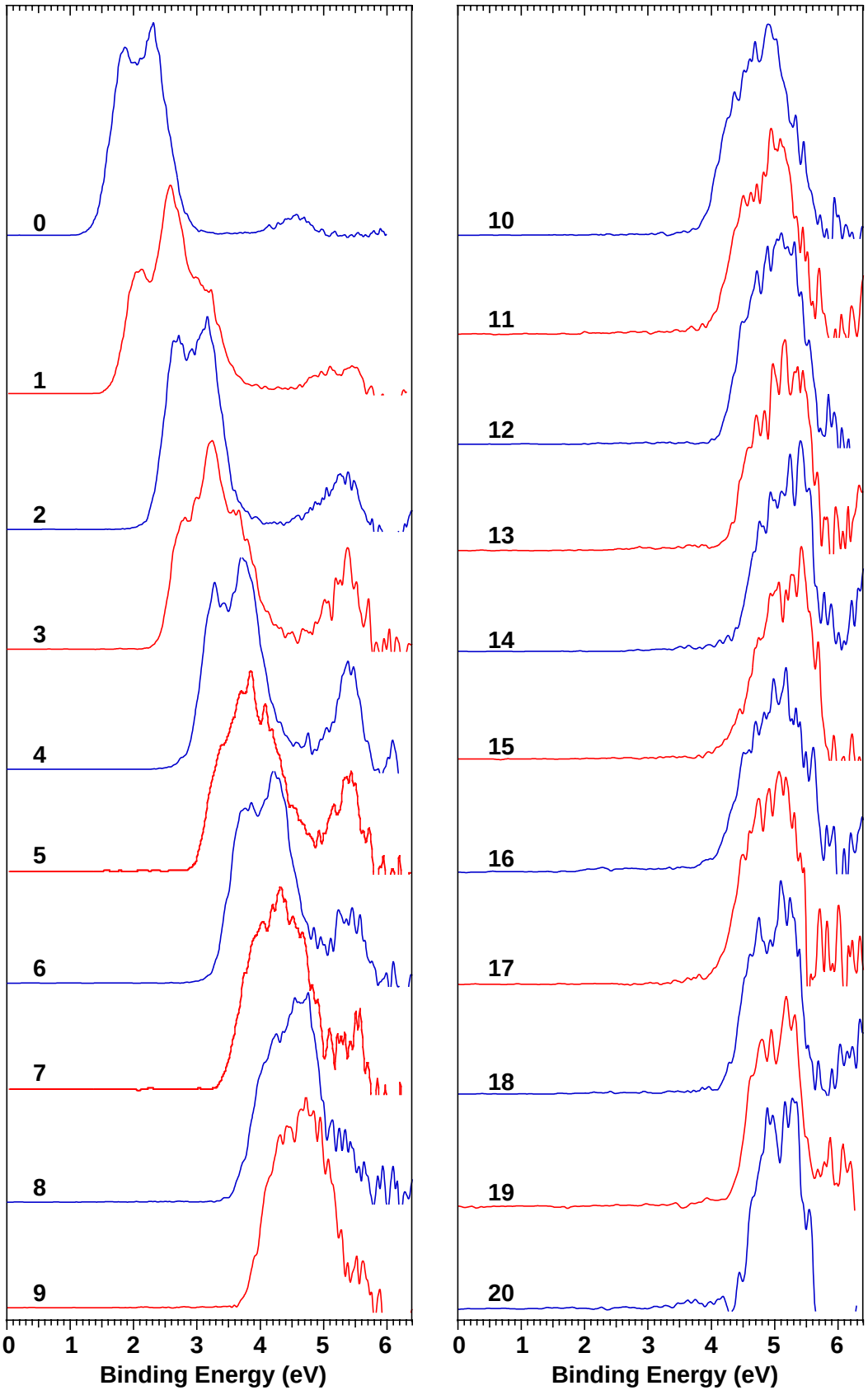
0
1
2
3
4
5
6
7
8
9
10
11
12
13
14
15
16
17
18
19
20
0 1 2 3 4 5 6
Binding Energy (eV)
0 1 2 3 4 5 6
Binding Energy (eV)

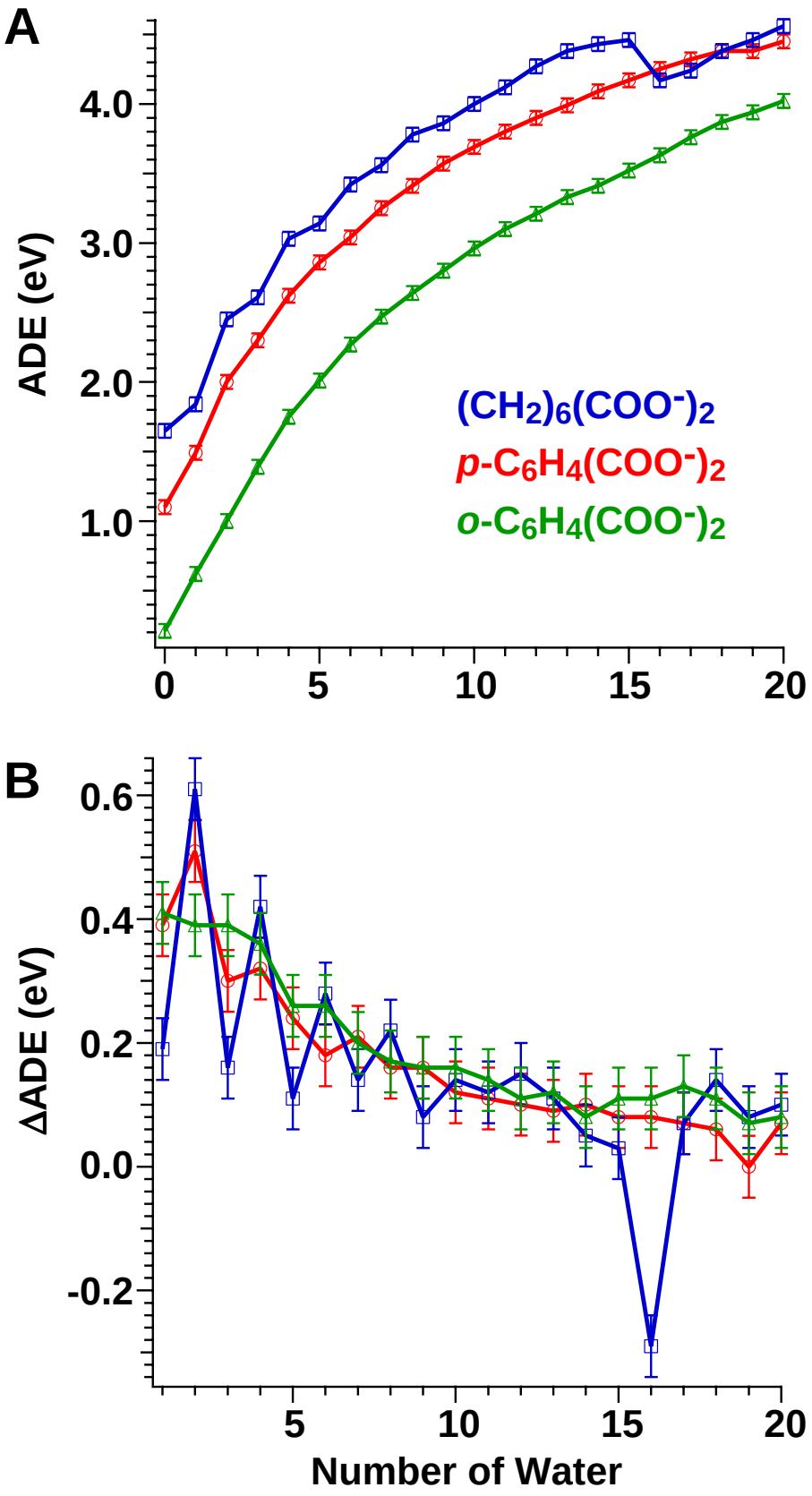
A
ADE (eV)
4.0
3.0
2.0
1.0
0
5
10
15
20
$(CH_2)_6(COO^-)_2$
p-$C_6H_4(COO^-)_2$
o-$C_6H_4(COO^-)_2$
B
ΔADE (eV)
0.6
0.4
0.2
0.0
-0.2
5
10
15
20
Number of Water

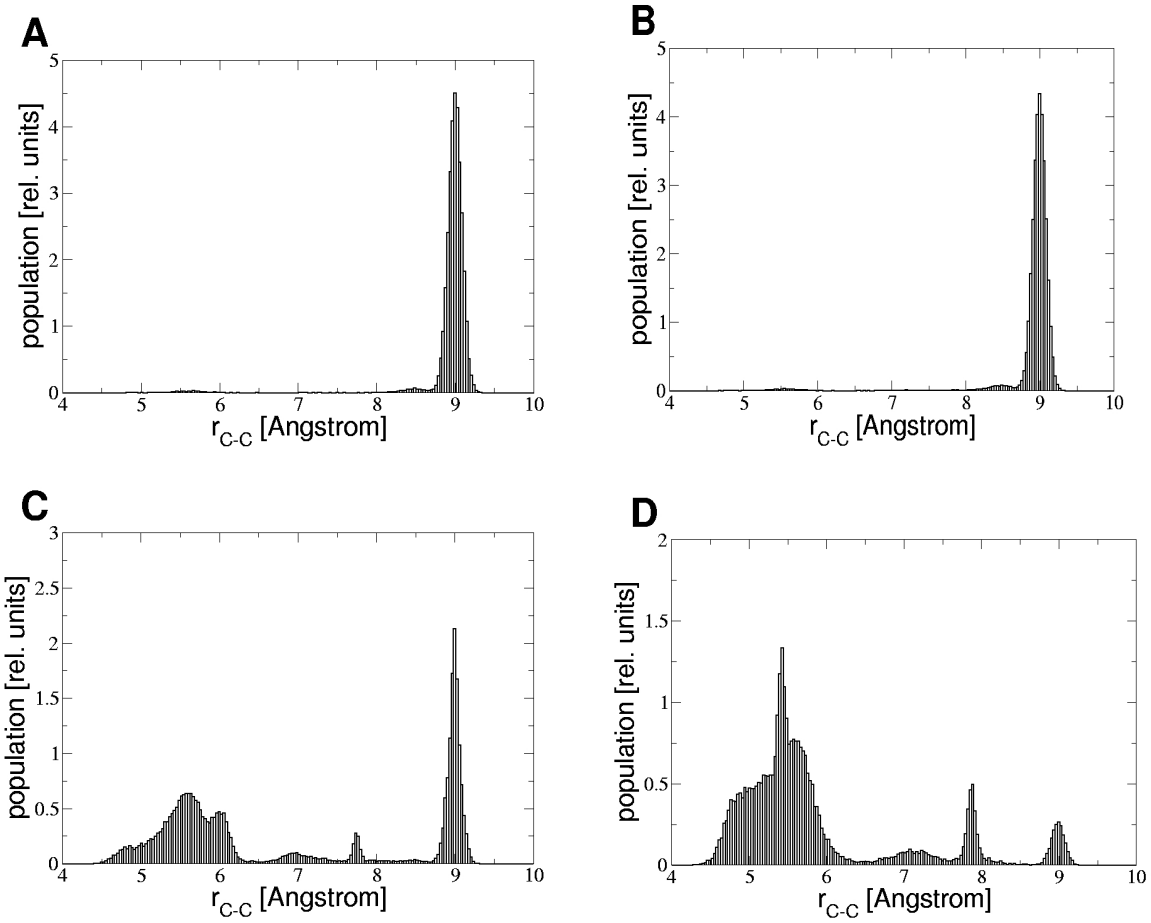
A
population [rel. units]
r C-C [Angstrom]
B
population [rel. units]
r C-C [Angstrom]
C
population [rel. units]
r C-C [Angstrom]
D
population [rel. units]
r C-C [Angstrom]

A

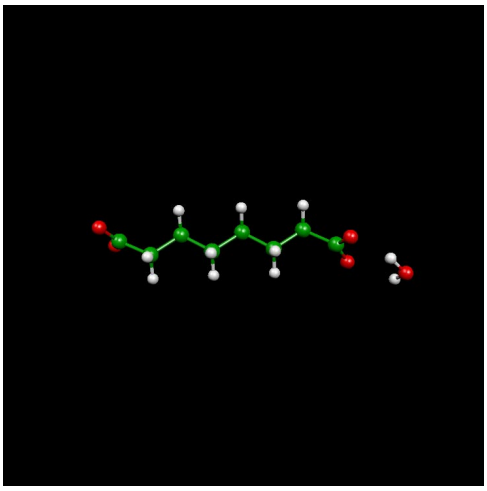

B

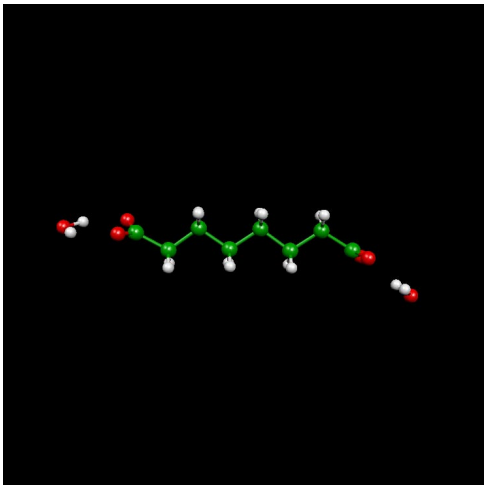

C

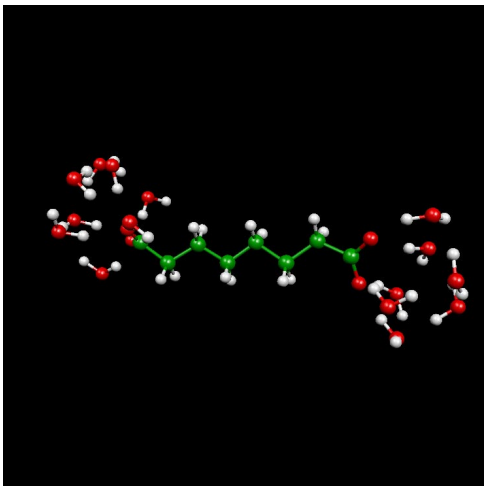

D

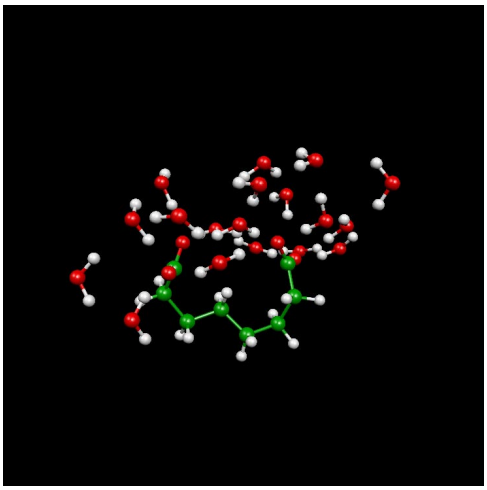

Graphics for table of content: